RSC Advances

PAPER

Cite this: *RSC Adv.*, 2020, **10**, 4832

Hydrophilic SiC hollow fiber membranes for low fouling separation of oil-in-water emulsions with high flux

Man Xu,[ab] Chenxi Xu,[a] K. P. Rakesh,[a] Yuge Cui,[a] Jun Yin,[a] Changlian Chen,[ab] Shulin Wang,[ab] Bingcai Chen[a] and Li Zhu *[ab]

The dry-wetting spinning technique involving immersion-induced phase inversion and dry-sintering was applied to prepare two types of SiC and Al_2O_3 hollow fiber membranes. The two hollow fiber membranes were characterized in terms of morphology and chemical surface composition by scanning electron microscopy (SEM), X-ray photoelectron spectroscopy (XPS), water contact angle and zeta potential measurements. The filtration capabilities of the two hollow fiber membranes were assessed by the separation of 200 mg L^{-1} synthetic (O/W) emulsions. During the treatment of O/W emulsions, the permeation flux of the SiC hollow fiber membrane was 163.9 L h^{-1} m^{-2}, which was higher than that of the Al_2O_3 hollow fiber membrane (139.4 L h^{-1} m^{-2}) at the beginning of the experiment. The membrane surface properties and the filtration results of O/W emulsion microfiltration demonstrated that the SiC hollow fiber membranes with a higher hydrophilicity had higher water flux and better anti-fouling properties.

Received 25th August 2019
Accepted 21st December 2019

DOI: 10.1039/c9ra06695k

rsc.li/rsc-advances

1. Introduction

Large amounts of oily wastewater pollution are being produced by industrial and residential applications, leading to a global risk for the environment and human health.[1–3] Lots of oil-in-water pollutants exist in emulsion form (O/W emulsions) and O/W emulsions are the most difficult to remove effectively, so O/W emulsion separation has double significance in ecology and economics.[4]

Membrane separation technology has become an emerging technology for the treatment of O/W emulsions due to merits such as high flux, low reprocessing cost, less energy consumption, and less environmental pollution.[5] Nowadays, inorganic and polymeric membranes have been successfully employed for the separation of O/W emulsions.[6] However, the main drawback of polymeric membranes in O/W emulsion treatment is their inherent hydrophobicity resulting in a high fouling tendency, which often leads to flux decrease in membrane performances.[7] Membrane fouling (including reversible and irreversible fouling) leads to the severe decline of permeate flux and thus compromises the membrane performance. Accordingly, mechanical and chemical cleaning is ultimately required.[1] In the direction of mitigate membrane fouling problems, one of the solutions is to develop a hydrophilic membrane which provides an enhanced hydrophilic character of membrane surface that can resist oil attachment and thus effectively prohibit permeation flux decline.[8]

Ceramic membranes made from ceramic powders including Al_2O_3, TiO_2, ZrO_2, are considered to be superior to polymeric membranes for the treatment of oily wastewater as they have improved hydrophilicity.[9–12] As such, there is a growing interesting in using inorganic membranes for purifying O/W emulsions in recent years.[13,14] However, like polymeric membranes, ceramic membranes also suffer from fouling during the treatment of O/W emulsions more or less.[15] The performance of ceramic membranes for O/W emulsions treatment must be continually improved. In this process, more hydrophilic membrane material and preparation technologies toward making ceramic membranes with good antifouling properties should be developed.[16]

Compared with polymeric and ceramic membranes (oxide materials membrane, such as Al_2O_3, TiO_2, and ZrO_2), SiC membranes are very hydrophilic.[17–19] Therefore, SiC membranes[20] have a high potential for oil separation and oily wastewater treatment applications because of their hydrophilicity, superb fouling resistance, and chemical stability.[21] SiC membranes have various configurations such as flat, tubular,[22] and hollow fibers.[23] For large scale applications, the hollow fiber configuration has higher packing density and higher water flux compared to the flat membrane.[24,25] However, few reports regard the O/W emulsions separation using the SiC hollow fiber membrane, not to mention the effect of surface property on the

[a]School of Materials Science and Engineering, Wuhan Institute of Technology, Wuhan, Hubei, China, 430073. E-mail: lzhu@wit.edu.cn; Fax: +86-27-87905136; Tel: +86-27-87905136

[b]Engineering Research Center of Environmental Materials and Membrane Technology of Hubei Province, Wuhan, Hubei, China, 430073

SiC hollow fiber membrane filtration performance in the treatment of O/W emulsions separation process.

In the present study, two types of SiC and Al_2O_3 hollow fiber membranes were prepared through the dry-wetting spinning technique involving immersion-induced phase inversion and dry-sintering method to mitigate the fouling of ceramic membranes in O/W emulsions treatment. The performance and fouling of the membranes by separation of O/W emulsions are compared under the same cross-filtration conduction and backwash procedure thus to obtain a better understanding of the relationship between the membrane fouling and surface property of the SiC hollow fiber membranes and Al_2O_3 hollow fiber membranes, thus to provide new insight into the membrane fouling control.

2. Material and methods

2.1 Fabrication and characterization of SiC and Al_2O_3 hollow fiber membranes

Commercially available SiC powders (purchased from Zhengzhou Lifeng, Abrasive Tools Co., Ltd) and Al_2O_3 powders (purchased from Nanjing Tansail Advanced Materials Co., Ltd) with an average particle diameter of 3.54 μm and 3.09 μm were used for the preparation of SiC and Al_2O_3 hollow fiber membranes. Polyethersulfone (PESf, Technical Pure, Radel A-100, Solvay Advanced Polymers, L. L. C.), *N*-methyl-2-pyrrolidone (NMP, Chemical Pure, Sinopharm Chemical Reagent Co., Ltd, China) and polyvinylpyrrolidone (PVP, Chemical Pure, Sinopharm Chemical Reagent Co., Ltd, China) were used as the binder, the solvent, and the additive, respectively.[26,27] PVP as an additive was introduced into the solution to modulate the suspension viscosity. Tap water was used as the internal and external coagulant.

2.1.1 Preparation of SiC and Al_2O_3 hollow fiber membranes. Polyethersulfone (PES, 9 wt%) and polyvinylpyrrolidone (PVP, 1 wt%) were dissolved in *N*-methyl-2-pyrrolidone (NMP, 35 wt%). After the polymer mixture solution was formed, the SiC powders or Al_2O_3 powders (50 wt%) was added into the solution and then milled for 12 h. The as-prepared suspension was degassed for 0.5 h and then extruded through a tube-in-orifice spinneret (outer diameter 2.5 mm, inner diameter 1.3 mm) using pressurized nitrogen gas (0.03 bar), and tap water were pumped through the bore of the spinneret as shown in Fig. 1. The fluid rate of the internal coagulant was 20 mL min^{-1}. After passing an air gap of 10 cm, the green hollow fiber bodies were immersed in a water bath for 24 h to allow the completion of the phase inversion process. The fibers were then dried at room temperature. The mass loss of

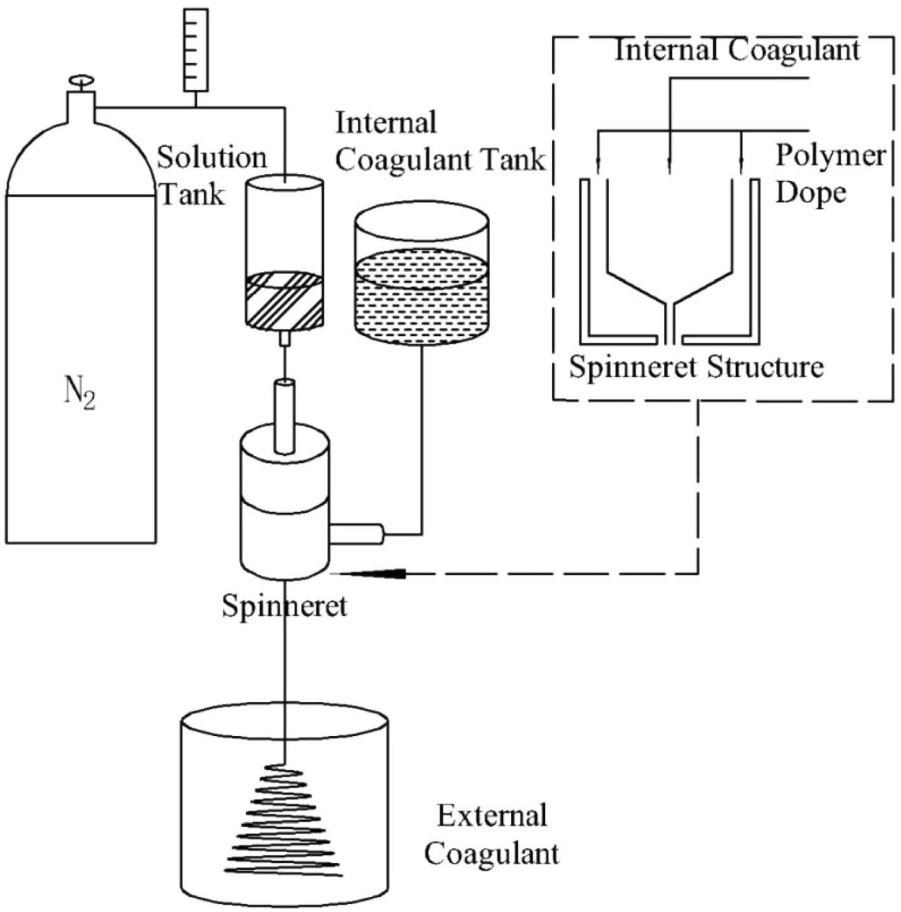

Fig. 1 Schematic diagram of the experimental set-up for the fabrication of hollow fiber membranes.

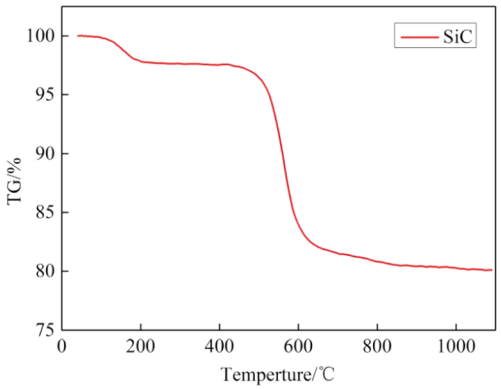

Fig. 2 TG data of SiC green hollow fiber membrane under air atmosphere.

the green SiC hollow fiber was shown in Fig. 2 under air atmosphere, at 100–220 °C, a minor mass loss was recorded that was accompanied by the release of water. A second mass loss step was recorded at 420–800 °C, this observed decomposition process matched closely to the reported decomposition of PES and PVP under an air atmosphere,[28,29] there was no obvious mass loss step after 800 °C, which indicated that organic matters were almost burned out at 800 °C. So the green SiC hollow fiber membrane was first heated under air atmosphere at 800 °C for 2 h to remove the organic polymer binder and additive, then sintered under argon atmosphere for 2 h at temperatures of 2050 °C using a high-temperature sintering furnace (NT/KGPS-160-1S, Changsha Nuotian Electronic Technology Co., Ltd) to avoid to be oxidized under air atmosphere at high temperature.[30] The green Al_2O_3 hollow fiber membrane was sintered at 1500 °C for 2 hours under air atmosphere. (KSL-1600, HeFei KeJing Materials Technology Co., Ltd).

2.1.2 Characterization. The morphologies of SiC and Al_2O_3 hollow fiber membranes were comparatively observed by Scanning Electronic Microscopy (SEM, JSM-5510LV, JEOL Ltd, Japan). The crystalline phase was determined *via* X-ray diffraction (XRD, D8 ADVANCE, Bruker Inc., Germany). Thermogravimetric analysis (TG) was conducted under air atmosphere with a heating rate of 20 °C min^{-1} using a Netzsch TG STA449F3 (Netzsch, German). The pore size distributions of SiC and Al_2O_3 hollow fiber membranes were measured by a pore size distribution analyzer (Porolux™ 500, Porometer, Germany) based on a gas–liquid displacement method. The pore diameter can be calculated from Washburn's equation using the bubble-point method.[31]

$$d = (4\gamma \cos \theta)/\Delta p \quad (1)$$

where γ is the surface tension coefficient of the liquid, θ is the contact angle of the liquid on the pore wall and Δp is the applied pressure difference.

The mechanical strength of the SiC hollow fiber membrane was measured by the three-point bending strength method using a universal testing machine (AGS-X, Shimadzu Ltd, Japan). The bending strength, (σ_f) was calculated based on the following equation.[32]

$$\sigma_f = 8FLd/\pi(D^4 - d^4) \quad (2)$$

where F is the measured force when a fracture occurs, L is the span, D and d stand for the outer and inner diameters of the hollow fiber, respectively.

Zeta potential was measured with a zeta potential analyzer (Malvern Nano ZSE, ZSW3700). Surface chemical properties characterization were carried out by X-ray photoelectron spectroscopy (XPS, Thermo Scientific Escalab 250, Thermo Fisher Scientific Inc., USA), The water contact angles for SiC and Al_2O_3 hollow fiber membranes were determined using a Kruss DSA 100 apparatus (Kruss Company, Ltd, Germany).

2.2 Microfiltration experiments

2.2.1 Preparation and separation of O/W emulsions. Synthetic O/W emulsions with a concentration of 200 mg L^{-1} were prepared using soybean oil (Shandong Luhua Group Co., Ltd) and Milli-Q water (Milli-Q Advantage A10, EMD Millipore Corporation, Germany). Then after ultrasonication of the mixtures for 6 h, a white and milky solution was produced. The size of O/W emulsions droplets was measured by the Malvern Mastersizer Analyzer (Mastersizer 2000, Malvern Instruments Ltd, UK). The stable O/W emulsions after 24 h had an average droplet size of 1.36 μm.

2.2.2 Microfiltration application of O/W emulsions. A lab-scale cross-flow membrane separation system was employed. The membrane filtration area was 1.0×10^{-4} m^2, cross flow velocity was 0.15 m s^{-1}, transmembrane pressure was 0.25 bar, respectively. The permeate water was collected and monitored on an electronic balance, which was used to calculate the permeate flux. The experiment was repeated twice. After a microfiltration test, the two hollow fiber membranes were cleaned by soaking in NaOH solutions (0.1 wt%) for a minimum of 2 h. Afterward, the hollow fiber membranes were rinsed with millipore water.

The trans-membrane permeate flux was calculated by the eqn (3)

$$F = V/At \quad (3)$$

where F is the permeate flux (in L m^{-2} h^{-1}), V is the volume of the permeate flow (in L), A is the surface area of the membrane (in m^2), and t is the filtration time (in h).

Rejection rate (R), measured by UV-visible spectrophotometer (UV-3600, Shimadzu, Japan), and was calculated by eqn (4),

$$R = ((C_F - C_P)/C_F) \times 100\% \quad (4)$$

where C_F and C_p are the concentrations in feed and permeate flow, respectively.

Flux recovery rate of each cycle (FR) was calculated with eqn (5), which represents the recovery extent of membrane permeability after back wash.

$$FR = F_1/F_0 \times 100\% \quad (5)$$

F_1 denotes the initial permeate flux after back wash, and F_0 is the origin permeate flux of the hollow fiber membranes. Higher

flux recovery rate indicates better antifouling performance and less fouling of the hollow fiber membrane. The higher the FR, the less the membrane is irreversibly fouled.

3. Results and discussion

3.1 Fabrication of the SiC and Al_2O_3 hollow fiber membrane

The XRD patterns showed that the peak of alumina was observed sintered at 1500 °C in Fig. 3, and the XRD data also provided a only 6H–SiC structure accompanied by no impurity or no secondary phase, so the pure SiC hollow fiber membrane was attained.

The colors of the SiC and Al_2O_3 hollow fiber membranes were seen in Fig. 4A, the SiC hollow fiber membrane was black, and the Al_2O_3 hollow fiber membrane was white. Fig. 4B shows the digital image of the prepared SiC and Al_2O_3 hollow fiber membranes in well-shaped hollow fiber configurations. The outer and inner diameters (OD/ID) (measured using Digital Microscopy Image Analyzer (DMIA) software) of the sintered SiC and Al_2O_3 hollow fiber membrane were measured at approximately 2.0 mm/1.7 mm and 2.5 mm/2.0 mm, the wall thickness of the two hollow fiber membrane was 0.3 mm and 0.5 mm respectively. The wall thickness of the two hollow fiber was much smaller than that of the ceramic tube membrane (1.5 mm),[33] resulting in a high membrane area per volume and thin thickness, which would be beneficial to improve the permeation flux through the hollow fiber membranes. As shown, the hollow fiber membranes possessed an asymmetric structure (Fig. 4C), sponge-like structure in the middle, sandwiched by a finger-like structure near the outer and inner walls. The finger-like layer extends from the inner surface across approximately 43% of the fiber, but layer length at the outer surface has been greatly reduced to 24%. A sponge-like region occupying approximately 33% of the fiber was present between the inner and outer finger-like voids. The larger lumen of the membrane was favorable to the fluid flow inside the lumen with less resistance.[34] From a close examination at the sponge-like structure region, as shown in Fig. 4D at high magnification, the surface of the SiC and Al_2O_3 hollow fiber membrane, packed by micrometer-sized SiC and Al_2O_3 particle, was uniform and smooth. The three point bending strength of the SiC hollow fiber membrane sintered at 1800 °C was 88.2 ± 2.5 MPa, which was comparative to the strength (85.8 ± 3.1 MPa) of Al_2O_3 hollow fiber sintered at 1500 °C in our previous study.[32] But the mechanical strength of the hollow fiber sintered at 1800 °C was lower compared to the strength of the tube, in order to impart the fiber with sufficient mechanical strength for practical applications, the 2050 °C calcination temperature was applied to obtain to a higher three point bending strength, which was 102.3 ± 6.7 MPa.

The pore size distributions of the membranes were shown in Fig. 5. It was observed that the two hollow fiber membranes possessed a uniform and narrow pore size distribution, meanwhile, the average pore size of the SiC and Al_2O_3 hollow fiber membranes were found to be 0.71 μm and 0.82 μm (Fig. 5).

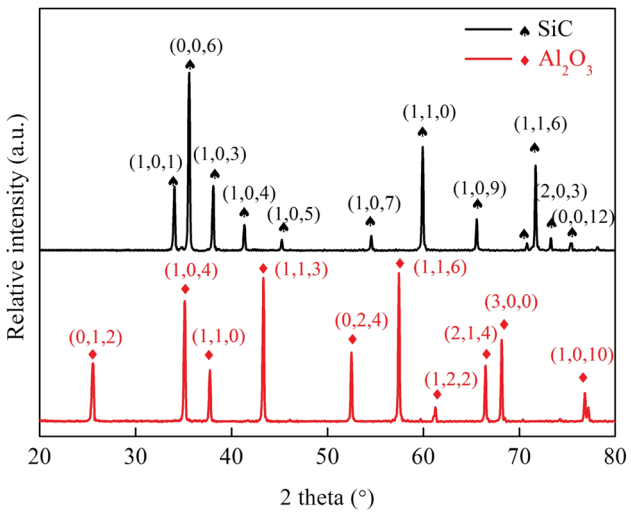

Fig. 3 XRD patterns of Al_2O_3 hollow fiber membrane sintered at 1500 °C and SiC hollow fiber membrane sintered at 2050 °C.

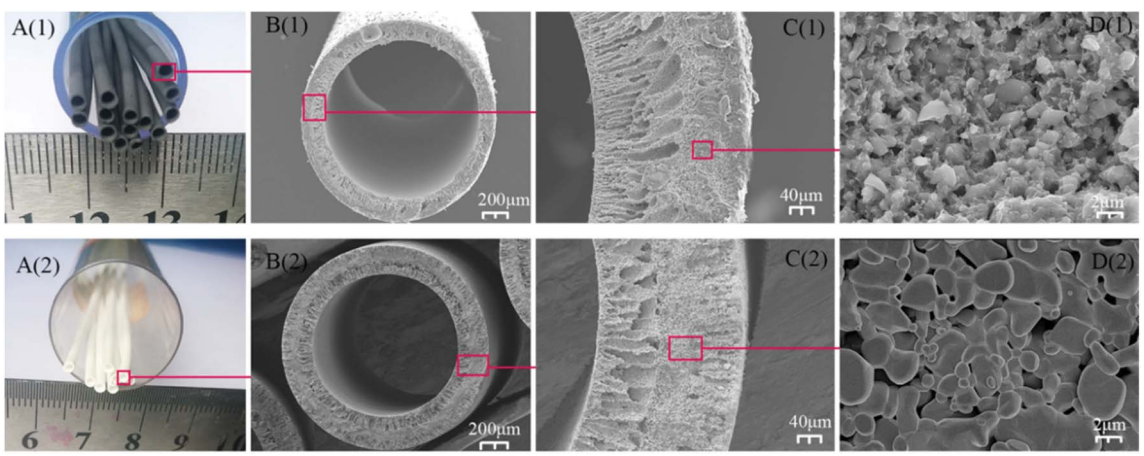

Fig. 4 (A) Digital image, (B) overall cross-sectional SEM image, (C) local enlarged cross-sectional SEM image, and (D) SEM image of porous structure of SiC hollow fiber membranes (A(1)–D(1)) and Al_2O_3 hollow fiber membranes (A(2)–D(2)).

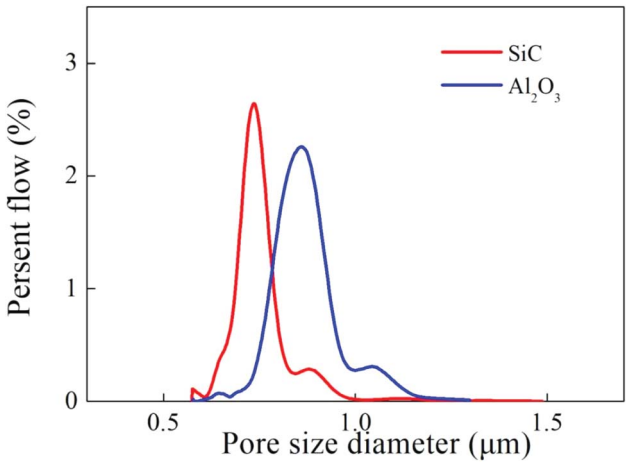

Fig. 5 The Pore size distribution of the SiC and Al_2O_3 hollow fiber membranes.

3.2 Hollow fiber membrane surface properties

Surface properties were characterized in terms of surface charge, surface hydroxyl groups and hydrophilicity.

3.2.1 Surface charge. Surface charge of membrane material influences electrostatic interactions between the membrane and the solutes.[35] Membrane fouling can be enhanced or reduced through electrostatic interactions, the surface charge of the ceramic membrane is developed through protonation/deprotonation of surface hydroxyl groups, which is pH-dependent.[36] The membrane surface shows a positive charge at pH < IEP (isoelectric point, the point where the zeta potential of the powders is zero) and a negative charge at pH > IEP. The zeta potential analysis of O/W emulsions at different pH values was presented in Fig. 6. The IEP was calculated at about 5.8 and 2.9 for the SiC powders and Al_2O_3 powders respectively, which are given by the intersection of the curves with the zeta potential axis.

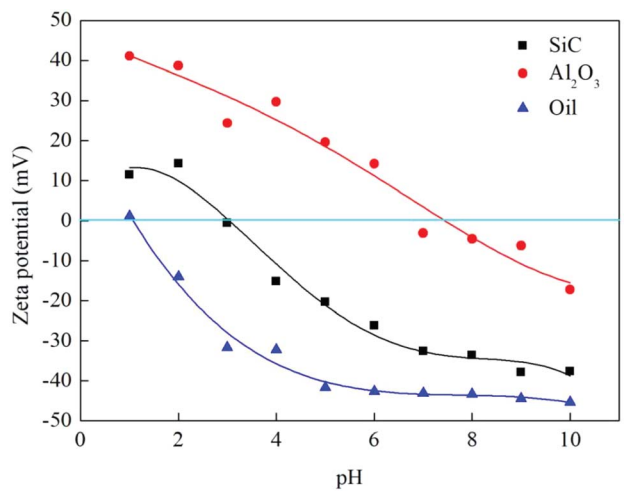

Fig. 6 Zeta potential for SiC powders, Al_2O_3 powders, and O/W emulsions as a function of pH.

At pH 6.5 (the pH of the emulsions) of the experiments, SiC hollow fiber membranes were negatively charged, whereas Al_2O_3 hollow fiber membranes were positively charged, oil droplets were negatively charged (Fig. 6), electrostatic repulsion between oil droplets and the SiC hollow fiber membrane surface would occur, while electrostatic attraction would exist between oil droplets and the Al_2O_3 hollow fiber membrane surface. The SiC hollow fiber membrane was expected to be excellent in antifouling ability due to its low isoelectric point (pH = 2.9). Hence, it can be inferred that SiC hollow fiber membrane can reduce the adsorption of undesired oil on the membrane surfaces and enhance the flux *via* reducing membrane fouling.

3.2.2 Surface hydroxyl groups. Fig. 7 shows the high-resolution XPS spectra of the O 1s region, taken on the surface of the SiC and Al_2O_3 hollow fiber membrane. Three deconvoluted signals of O 1s peak could be assigned to three oxygen-related species: adsorbed oxygen-containing species (at ~534.3 eV), lattice oxygen ions O^{2-} (at ~535.0 eV), and surface hydroxyl groups (–OH group, at ~535.6 eV) respectively.[13]

For the Al_2O_3 hollow fiber membrane, *via* quantification of O 1s peak, the content of contained surface OH- groups was estimated to be 11.6%. By comparison, a substantial increase in surface –OH groups amount was achieved for SiC hollow fiber membranes' surface (20.1%), which might be due to the presence of more adsorbed water molecules from the atmospheric environment, as the top-layer of the SiC hollow fiber membrane was very hydrophilic.[16,37] Therefore, the surface OH- groups of SiC hollow fiber membrane probably tend to interact strongly with water molecules through a hydrogen bond, whereas those of the Al_2O_3 hollow fiber membrane would be significantly less hydrophilic. This hypothesis will be confirmed in the following hydrophilicity test.

3.2.3 Hydrophilicity. Hydrophilicity was an important parameter for predicting the fouling tendency of filtration membranes.[38] The hydrophilicity of the two hollow fiber membranes used in this study was tested with water contact angle measurement. The contact angles of the SiC and Al_2O_3 hollow fiber membranes were 11.3° and 23.4° respectively. In general, a small contact angle indicated high hydrophilicity of the material, high hydrophilicity usually meant low membrane fouling potential infiltration process. The stronger hydrophilic SiC hollow fiber membranes surface was expected to repel oil droplets from adhering onto it, thus to weaken membrane fouling during separation treatment of O/W emulsions.

3.3 Membrane separation of O/W emulsions

The photographs of the O/W emulsions and the collected permeate separated by the SiC hollow fiber membranes were shown in Fig. 8. The O/W emulsions were milky white because of the light scattering by oil spheres. The collected permeate was clear and transparent, as shown in the optical microscopy images, no obvious droplets could be observed in the filtrates, indicating that the large oil droplets were effectively cut off. The size distribution of the oil droplets in the O/W emulsions was at approximately 1.36 μm, and the pore size of the SiC hollow fiber membranes (0.71 μm) was very small compared to the size of oil.

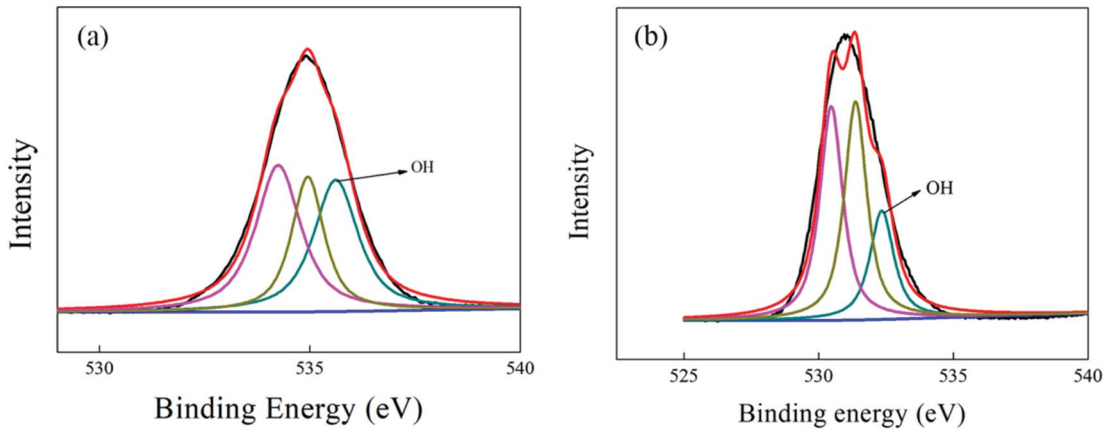

Fig. 7 XPS depth profile spectra of the O-1s peaks for the surface of SiC hollow fiber membrane (a) and Al_2O_3 hollow fiber membrane (b).

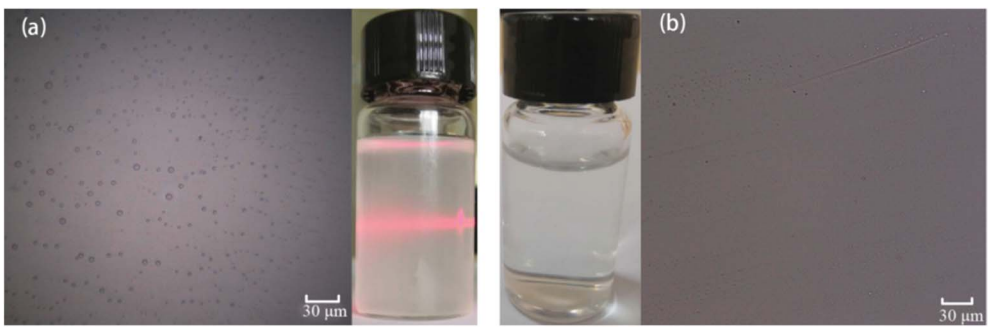

Fig. 8 Photographs and optical microscopy images of O/W emulsions (a) and the permeate (b) separated by the SiC hollow fiber membranes.

The results indicated that the SiC hollow fiber membranes fabricated in this study could separate O/W emulsions effectively through a sieving mechanism.

The permeabilities of the O/W emulsions using the two hollow fiber membranes were investigated as illustrated in Fig. 9. The permeation flux of the SiC hollow fiber membrane was 163.9 L h^{-1} m^{-2}, which was higher compared to the Al_2O_3 hollow fiber membrane of 139.4 L h^{-1} m^{-2} at the beginning of the experiment. The permeation flux of the SiC hollow fiber membrane was 103.9 L h^{-1} m^{-2} after 150 min operation, which was also higher than the Al_2O_3 hollow fiber membrane's permeation flux of 57.1 L h^{-1} m^{-2}. As shown in Fig. 9, the two membranes all suffered a permeate-flux decline of different extent during filtration, which can be ascribed to membrane fouling. The fouling of the two hollow fiber membranes was typically formed by oil droplets present in the O/W emulsions, the average particle size of the oil was at approximately 1.36 μm, a small fraction of the particle size of the oil droplets was smaller than 1.36 μm, which was also smaller than the pore size of the SiC hollow fiber membranes (0.71 μm), at the beginning of the filtration, the small fraction smaller oil droplets could directly penetrated and stuck inside membrane pores. But the majority of the oil particle cannot permeate through the membranes, and water molecules were allowed to permeate through the membrane pores. However, the SiC hollow fiber membranes showed slower flux reduction ration than the Al_2O_3 hollow fiber membrane, only ~36.7% for the SiC hollow fiber membrane, and as high as ~59.1% for Al_2O_3 membranes during the 150 min period operation. In this study, the Hermia model[39] was employed to identify the fouling mechanism in the filtration of O/W emulsion using the SiC hollow fiber membrane. It is concluded that, at the first stage of membrane filtration process (t < 75 min), the oil droplets adhered easily onto the membrane surface where an intermediate pore blocking occurred, thus decreasing the permeation flux significantly.

The SiC hollow fiber membranes had stronger hydrophilic than the Al_2O_3 hollow fiber membranes, thus the blocking of membrane pore was avoided because the hydrophilic membrane pores had a high capillary repulsing force to prevent oil droplets from transporting across.[13] Moreover, owing to the characteristic negative charge on the material surface and oil particle as described in Section 3.2.1, the ability to reduce deposition of oil foulants was highly increased.[40,41] Although there was repulsion between the negatively charged oil droplets and the membrane surface, the tiny oil droplets were more likely to be squeezed into membrane pores under pressure. The penetration of the tiny oil droplets into the membrane pores probably led to membrane fouling. In contrast, the Al_2O_3 hollow fiber membrane was less hydrophilic, resulting in stronger adsorption of oil droplets on the membrane surface.[14]

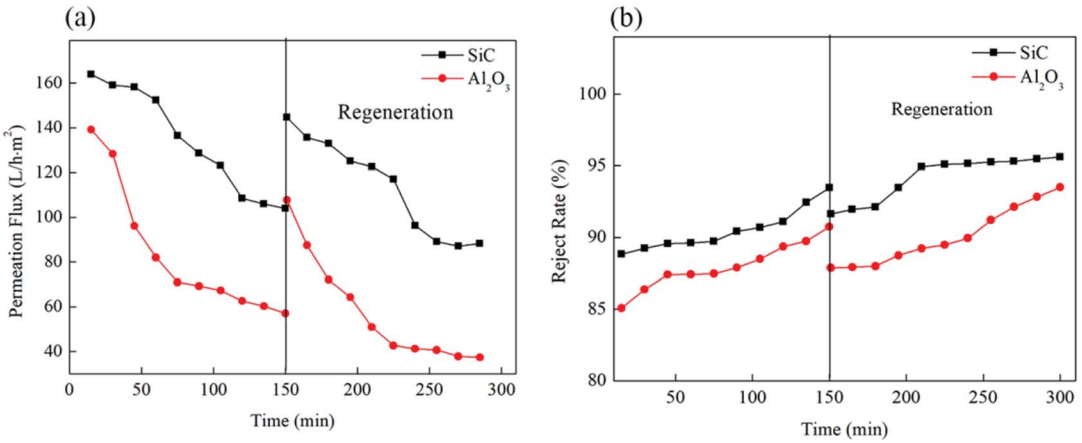

Fig. 9 Variation of permeation flux and oil rejection rate with time during membrane filtration of O/W emulsions using the two hollow fiber membranes regeneration for two runs *via* a back-flushing of 0.1 wt% NaOH aqueous solution.

Table 1 Comparison between permeation fluxes for the as-fabricated SiC hollow fiber membrane in this work and those reported in the literatures

Membrane			Performance			
Material	Pore size	Water contact angles	Configuration	Normalized flux ($L\ h^{-1}\ m^{-2}\ bar^{-1}$)	Rd (%)	Ref.
SiC	0.71	11	Hollow fiber	654	93.5	This work
SiC	0.25	—	Tubular	200	—	19
Si_3N_4	0.68	—	Hollow fiber	260	91	39
TiO_2–mullite	0.11	11	Hollow fiber	150	97	2
TiO_2–Al_2O_3	6	8	Tubular	320	>99	14

Flux recovery rate (FR) represents the recovery extent of membrane permeability after backwash. Higher FR indicated better antifouling performance and less fouling of the ceramic membrane. These two hollow fiber membranes had different FR after two filtration cycles. For the SiC hollow fiber membrane, it was realized to recover up to 144.7 $L\ h^{-1}\ m^{-2}$, the FR over 88.3% of the original flux 163.9 $L\ h^{-1}\ m^{-2}$ by backwashing. This result demonstrated that most of the fouling was removed by a hydraulic backflush. The SiC hollow fiber membrane with alkalescent water soaking can be a promising technology to reduce the fouling of the hollow fiber membranes and enhance membrane cleaning efficiency in the treatment of O/W emulsions. For the Al_2O_3 hollow fiber membrane, membrane fouling reduced the FR by 77.4%. This was probably because the Al_2O_3 hollow fiber membrane suffered much more irreversible adsorption fouling than the hydrophilic SiC hollow fiber membrane. This fact again confirmed that the hydrophilicity was a more significant factor influencing the membrane fouling tendency of the membrane in O/W emulsions treatment. This could also be seen as a confirmation of the hypothesis that the SiC hollow fiber membranes with the stronger hydrophilicity had higher water flux and the better anti-fouling property.[19,42]

Fig. 9 also shows the variation of the oil rejection rate using the two hollow fiber membranes. As shown in Fig. 9, 90.7% of the oil rejection rate was obtained by positively charged Al_2O_3 hollow fiber membrane, whereas the rejection rate was 93.5% of the negatively charged SiC membranes. These results indicated a higher oil rejection for the SiC hollow fiber membrane compared with that of the Al_2O_3 hollow fiber membrane in the whole process. In general, oil rejection can be enhanced if the membrane was oppositely charged. Therefore, the produced hydrophilic SiC hollow fiber membranes, which exhibited excellent permeability and high oil rejection, can be suggested for O/W emulsions treatment. When compared with reported data in literatures in Table 1.[2,14,19,43] It shows that SiC hollow fiber membrane shows superior results, which has the compared rejection rate, along with the highest flux.

4. Conclusion

A combined induced phase inversion-sintering technique was used for fabricating SiC and Al_2O_3 hollow fiber membranes. Pore size measurements showed that the pore size of the SiC and Al_2O_3 hollow fiber membranes were 0.71 μm and 0.82 μm respectively, which was similar to each other. The SiC hollow fiber membranes were more hydrophilic due to the higher surface site density of surface –OH group and lower water contact angle than the Al_2O_3 hollow fiber membrane. The filtration efficiency of the O/W emulsions results showed that the more hydrophilic SiC hollow fiber membranes contributed

to repel oil droplets from adhering to membrane surface, thus to weaken membrane fouling, the permeation flux of the SiC hollow fiber membrane (163.9 L h^{-1} m^{-2}) was higher compared to the Al_2O_3 hollow fiber membrane (139.4 L h^{-1} m^{-2}) at the beginning of the experiment. Dilute NaOH solution back-washing was used to effectively accomplish SiC hollow fiber membranes regeneration (~88.3% flux recovery rate). It was indicated that the SiC hollow fiber membranes with the stronger hydrophilicity had higher water flux and the better anti-fouling property owing to electrostatic repulsion to the oil during separation treatment of O/W emulsions.

Conflicts of interest

There are no conflicts to declare.

Acknowledgements

This work was financially supported by the Science Research Fund of Wuhan Institute of Technology (Grant No. 18QD06) and Project of Technology Innovation in Hubei Province (Grant No. 2016ACA161).

References

1 M. Hengyang, Q. Minghui, B. Jiawei, C. Xianfu, V. Henk and F. Yiqun, *ACS Appl. Mater. Interfaces*, 2018, **10**, 18093–18103.
2 L. Zhu, X. Dong, M. Xu, F. Yang, M. D. Guiver and Y. Dong, *J. Membr. Sci.*, 2019, **582**, 140–150.
3 Y. Yang, H. Wang, J. Li, B. He, T. Wang and S. Liao, *Environ. Sci. Technol.*, 2012, **46**, 6815–6821.
4 Y. Si and Z. Guo, *Chem. Lett.*, 2015, **7**, 874–883.
5 M. Padaki, R. Murali, M. Abdullah, N. Misdan, A. Moslehyani, M. Kassim, N. Hilal and A. Ismail, *Desalination*, 2015, **357**, 197–207.
6 S. Hosseinabadi, M. Reza Sebzari, M. Hemati, F. Rekabdar and T. Mohammadi, *Desalination*, 2011, **1–3**, 222–228.
7 M. C. Fraga, S. Sanches, V. J. Pereira, J. G. Crespo, L. Yuan, J. Marcher, M. V. M. de Yuso, E. Rodríguez-Castellón and J. Benavente, *J. Eur. Ceram. Soc.*, 2017, **37**, 899–905.
8 H. Abadikhah, J.-W. Wang, X. Xu and S. Agathopoulos, *J. Water Process. Eng.*, 2019, **29**, 100799.
9 A. Lee, J. W. Elam and S. B. Darling, *Environ. Sci.: Water Res. Technol.*, 2016, **2**, 17–42.
10 X. Hu, Y. Yu, J. Zhou, Y. Wang, J. Liang, X. Zhang, Q. Chang and L. Song, *J. Membr. Sci.*, 2015, **476**, 200–204.
11 F. L. Hua, Y. F. Tsang, Y. J. Wang, S. Y. Chan, H. Chua and S. N. Sin, *Chem. Eng. J.*, 2006, **128**, 169–175.
12 J.-E. Zhou, Q. Chang, Y. Wang, J. Wang and G. Meng, *Sep. Purif. Technol.*, 2010, **75**, 243–248.
13 L. Zhu, M. Chen, Y. Dong, C. Y. Tang, A. Huang and L. Li, *Water Res.*, 2016, **90**, 277–285.
14 Q. Chang, J.-E. Zhou, Y. Wang, J. Liang, X. Zhang, S. Cerneaux, X. Wang, Z. Zhu and Y. Dong, *J. Membr. Sci.*, 2014, **456**, 128–133.
15 D. Lu, T. Zhang and J. Ma, *Environ. Sci. Technol.*, 2015, **49**, 4235–4244.
16 L. Dongwei, Z. Tao, G. Leo, M. Jun and C. Jean-Philippe, *Environ. Sci. Technol.*, 2016, **50**, 4668–4674.
17 W. Deng, X. Yu, M. Sahimi and T. T. Tsotsis, *J. Membr. Sci.*, 2014, **451**, 192–204.
18 M. C. Fraga, S. Sanches, V. J. Pereira, J. G. Crespo, L. Yuan, J. Marcher, M. V. M. d. Yuso, E. Rodríguez-Castellón and J. Benavente, *J. Eur. Ceram. Soc.*, 2017, **37**, 899–905.
19 B. Hofs, J. Ogier, D. Vries, E. F. Beerendonk and E. R. Cornelissen, *Sep. Purif. Technol.*, 2011, **79**, 365–374.
20 S. Chang Kim, H.-J. Yeom, Y.-W. Kim, I.-H. Song and J.-H. Ha, *Int. J. Appl. Ceram. Technol.*, 2017, **14**, 692–702.
21 M. Fukushima, Y. Zhou, Y.-I. Yoshizawa and K. Hirao, *J. Eur. Ceram. Soc.*, 2008, **28**, 1043–1048.
22 Y. Zhou, M. Fukushima, H. Miyazaki, Y.-I. Yoshizawa, K. Hirao, Y. Iwamoto and K. Sato, *J. Membr. Sci.*, 2011, **369**, 112–118.
23 G. Xu, K. Wang, Z. Zhong, C.-S. Chen, P. Webley and H. Wang, *J. Mater. Chem. A*, 2014, **2**, 5841–5846.
24 H. Abadikhah, C.-N. Zou, Y.-Z. Hao, J.-W. Wang, L. Lin, S. Khan, X. Xu, C.-S. Chen and S. Agathopoulos, *J. Eur. Ceram. Soc.*, 2018, **38**, 4384–4394.
25 P. D. Wit, E. J. Kappert, T. Lohaus, M. Wessling, A. Nijmeijer and N. E. Benes, *J. Membr. Sci.*, 2015, **475**, 480–487.
26 B. F. K. Kingsbury and K. Li, *J. Membr. Sci.*, 2009, **328**, 134–140.
27 S. M. Liu and K. Li, *J. Membr. Sci.*, 2003, **218**, 269–277.
28 X. G. Li, H. T. Shao, H. Bai, M. R. Huang and W. Zhang, *J. Appl. Polym. Sci.*, 2003, **90**, 3631–3637.
29 Y. K. Du, P. Yang, Z. G. Mou, N. P. Hua and L. Jiang, *J. Appl. Polym. Sci.*, 2005, **99**(1), 23–26.
30 T. Narushima, T. Goto, T. Hirai and Y. Iguchi, *Mater. Trans. JIM*, 1997, **38**, 821–835.
31 G. Chen, H. Qi, W. Xing and N. Xu, *J. Membr. Sci.*, 2008, **318**, 38–44.
32 L. Zhu, J. Ji, S. Wang, C. Xu, K. Yang and M. Xu, *Chemosphere*, 2018, **206**, 278–284.
33 X. Tan, S. Liu and K. Li, *J. Membr. Sci.*, 2001, **188**, 87–95.
34 R. Wang, L. Shi, C. Y. Tang, S. Chou, C. Qiu and A. G. Fane, *J. Membr. Sci.*, 2010, **355**, 158–167.
35 J. Binner and Y. Zhang, *J. Mater. Sci. Lett.*, 2001, **20**, 123–126.
36 X. Ma, C. Pengli, M. Zhou, Z. Zhong, F. Zhang and W. Xing, *Ind. Eng. Chem. Res.*, 2017, **56**, 7070–7079.
37 M. Takeuchi, G. Martra, S. Coluccia and M. Anpo, *J. Phys. Chem. B*, 2005, **109**, 7387–7391.
38 S. J. Oh, N. Kim and Y. T. Lee, *J. Membr. Sci.*, 2009, **345**, 13–20.
39 H. Huang, T. A. Young and J. G. Jacangelo, *Environ. Sci. Technol.*, 2008, **42**, 714–720.
40 B. P. Singh, J. Jena, L. Besra and S. Bhattacharjee, *J. Nanopart. Res.*, 2007, **9**, 797–806.
41 S. Z. A. Bukhari, J.-H. Ha, J. Lee and I.-H. Song, *J. Eur. Ceram. Soc.*, 2018, **38**, 1711–1719.
42 H. Huang, T. Young and J. G. Jacangelo, *J. Membr. Sci.*, 2009, **334**, 1–8.
43 H. Abadikhah, C.-N. Zou, Y.-Z. Hao, J.-W. Wang, L. Lin, S. A. Khan, X. Xu, C.-S. Chen and S. Agathopoulos, *J. Eur. Ceram. Soc.*, 2018, **38**, 4384–4394.